Drop size distribution monitoring of oil-in-water emulsions in SMX+ static mixers: Effect of operating and geometrical conditions

Elodie Chabanon, Nida Sheibat-Othman, O. Mdere, Jean-Pierre Valour, Sébastien Urbaniak, François Puel

To cite this article: **E. CHABANON, N. SHEIBAT-OTHMAN, O. MDERE, J.P. VALOUR, S. URBANIAK, F. PUEL (2017) Drop Size Distribution Monitoring of Oil-in-Water Emulsions in SMX+ Static Mixers: Effect of Operating and Geometrical Conditions International Journal of Multiphase Flow 92 (June 2017), 61–69** http://dx.doi.org/10.1016/j.ijmultiphaseflow.2017.03.001

Drop Size Distribution Monitoring of Oil-in-Water Emulsions in SMX+ Static Mixers: Effect of Operating and Geometrical Conditions

E. Chabanon[a]*, N. Sheibat-Othman[a], O. Mdere[a], J.P. Valour[a], S. Urbaniak[a], F. Puel[b]

[a]Univ Lyon, Université Claude Bernard Lyon 1, CNRS UMR 5007, LAGEP, F-69622, Lyon, France.

[b]LGPM, Laboratoire de Génie des Procédés et Matériaux, CentraleSupélec, université Paris-Saclay, Grande voie des Vignes, 92295, Châtenay-Malabry, France

* : Corresponding author : tel. +33 4 72 43 18 52, E-mail: elodie.chabanon@univ-lyon1.fr

ABSTRACT

Static mixers provide enhanced mixing via a motionless element inside a rigid pipe, and are widely used for continuous mixing and blending in industry. This study focuses on the emulsification of a silicon oil-in-water system stabilized by a surfactant through SMX+® static mixers involving no mass transfer between the two phases. The experiments covered a large domain of dispersed fraction from dilute conditions (5 %vol.) up to concentrated ones (60 %vol.) close to phase inversion and three different viscosities from 20 to 350 mPa s with transitional or turbulent flow regimes. The number of static mixers was studied until a constant drop size distribution monitored at line with a video probe was obtained. With the considered flow rates, only the five first SMX+ elements were necessary to achieve a complete drop breakup and coalescence equilibrium, the following ones only causing a supplementary pressure drop. The influence of the number of SMX+ and energy dissipation rate was found to be of first order

compared to the volume fraction or viscosity of the dispersed phase. According to the large amount of data, it was possible to establish a new form of a Middleman correlation dedicated to this type of mixer of new generation. The formula takes into account the number of static mixers besides other hydrodynamic and physicochemical parameters.

KEYWORDS: Oil-in-water emulsions, SMX+ static mixers, viscous fluids, high volume fraction, Process Modelling

1. INTRODUCTION

The development of multiphase systems, such as mixing immiscible gas-liquid or liquid-liquid fluids, is one of the major challenges of engineering processes in different domains like cosmetic, pharmaceutical, chemical and food industries (Leng and Calabrese, 2003). Amongst them, Oil-in-Water (O/W) emulsions represent an important sub-group where the dispersed phase is organic, i.e. the oil, and the continuous phase is aqueous. Controlling the drop size distribution (DSD), at lower power consumption, is important in these systems as it might affect mass transfer and potential reactions during the formation as well as the quality of many finished emulsion products (Becker et al., 2014).

Emulsions can be realized using mechanical stirrers (such as turbines and rotor stators), high pressure homogenizers or static mixers. Stirred tanks are still assumed to be the reference for emulsification in most industrial applications because of their flexibility and the possibility of mixing viscous products which are difficult to pump. But, the emulsification efficiency is limited and spatially non-uniform (due to higher shear around the stirrer). Moreover, they suffer from space requirement, operating cost (OPEX) and capital cost (CAPEX), long residence-time distributions, non-isothermal operating condition and the decrease of safety conditions and process control due to the big volume (Ghanem et al., 2014). Consequently, the development of continuous processes have been promoted in order to reduce the size of the process unit, increase

the productivity, homogenize the shear rates, enhance heat transfer and allow faster scale-up from the lab-scale to the industrial-scale (Al Taweel et al., 2007; Ghanem et al., 2014; Laporte et al., 2014; Thakur et al., 2003; Van Gerven and Stankiewicz, 2009).

Static mixers allow continuous production with lower energy consumption than mechanical agitators (mainly compared to rotor stators or high pressure homogenizers) while maintaining good mixing performances (Anxionnaz et al., 2008; Bayat et al., 2012; Couvert et al., 2006; Thakur et al., 2003). They consist of small motionless elements, with complex porous structures. They are inserted in a pipe, where a fluid is pumped, to generate shear by redistributing the fluid in directions transverse to the main flow. The main energy consumption consists therefore of pumping the fluid in the unit, which increases with the pressure drop. The pressure drop thus and fluid velocity constitute the driving force for dispersing the two immiscible liquids when flowing through the mixing elements. Static mixing units require therefore optimization of energy (pressure drop, time and mixing length) as well as drop size. The mixing length is modified through the number of static mixers or the number of passes (that are equivalent if pumping effects are negligible).

Different designs of static mixers are available commercially, and the most widely used are Kenics® helical mixer from Chemineer (Berkman and Calabrese, 1988; Chen and Libby, 1978; Haas, 1987; Middleman, 1974; Yamamoto et al., 2007) and more recently SMV® (Paglianti and Montante, 2013) and SMX® static mixers from Sulzer. SMX static mixers were used for mixing miscible fluids, as well as non-miscible fluids (gas-liquid and liquid-liquid), either in laminar (Anxionnaz et al., 2008; Das et al., 2013, 2005; Fradette et al., 2007; Kiss et al., 2011; Laporte et al., 2014; Legrand et al., 2001; Liu et al., 2005; Rama Rao et al., 2007; Thakur et al., 2003) or turbulent regimes (Anxionnaz et al., 2008; Lobry et al., 2011; Streiff et al., 1997; Thakur et al., 2003; Theron et al., 2010; Theron and Sauze, 2011). SMX+ and SMX static mixers have the same X geometry but in SMX+ the crossed bars are thinner and less numerous which leads to a

reduction in the pressure drop to about 50 % compared to SMX (Hirschberg et al., 2009). SMX+ static mixers have already been used for liquid-liquid and gas-liquid systems (Baumann et al., 2012; Hirschberg et al., 2009; Laporte et al., 2014; Meijer et al., 2012; Theron and Sauze, 2011).

Understanding and modelling the mechanisms taking place in liquid-liquid emulsification using static mixers are still not completely achieved. This is due to the wide range of geometries and working conditions, such as the flow rates, flow regime (laminar to turbulent), surfactant dynamics, fluid type (Newtonian or non-Newtonian), volume fraction of the dispersed phase, or the ratios of densities and viscosities of the dispersed phase to the continuous phase. Due to the lack of complete experimental data, the available models are still not universal for the various static mixers and fluids. In particular, the available literature of liquid-liquid emulsification using static mixers is limited to dilute systems, with a dispersed phase volume fraction (Φ_d) rarely higher than 35 %vol. However, the increase of the dispersed phase volume fraction might have an effect on both the droplet size and the pressure drop, for instance due to an increase in the apparent viscosity (if the dispersed phase is more viscous than the continuous one).

This work aims to characterize oil-in-water emulsions through SMX+ static mixers involving no mass transfer between the two phases. It investigates the influence of the fluids viscosities and densities, the dispersed phase volume fraction (from diluted systems to highly concentrated ones), the Reynolds number (from transitional to turbulent flows) and the number of SMX+ static mixers on the drop size distribution and the Sauter mean diameters. These impacts are then described using a new optimized correlation. The correlation accounts thus for the number of mixers and hydrodynamic and physicochemical parameters.

2. MATERIALS AND METHODS

2.1 Emulsion ingredients

The investigated oil-in-water emulsions are made up of silicon oil, which constitutes the dispersed phase (supplied by Bluestar Silicone/France), and distilled water as the continuous phase. Three viscosities of silicon oils are studied, 20, 100 and 350 mPa s, hereafter denoted V20, V100 and V350 respectively. The emulsions are stabilized by the surfactant polyoxyethylene (20) sorbitan monolaurate (Montanox 20®), $C_{58}H_{114}O_{26}$ (supplied by SEPPIC). The physicochemical properties of the different fluids are summarized in Table 1.

2.2 Static mixers

The recently developed SMX+ static mixers (supplied by Sulzer, cf. Figure 1) are used in this work for their ability to limit the pressure drop and improve the mixing performance of viscous fluids (Hirschberg et al., 2009). Each element is composed of an array of crossed bars (6 in each direction) arranged at an angle of 45° relative to the flow direction. Note that SMX mixers have 8 crossed bars in each direction which causes higher pressure drop (Hirschberg et al., 2009). The diameter and the height of each SMX+ is about 5 mm, which results in an aspect ratio of length to diameter per static mixer of L/D = 1. They have a 75% global porosity (φ), a hydraulic diameter of D_h = 1.42×10^{-3} m (taking into account the tube walls) and a specific area of a_g = 1527 m^2 m^{-3} (neglecting the tube surface). The used mixers are made of stainless steel.

2.3 Experimental Setup

The used experimental set-up is described in Figure 2. The SMX+ static mixers are placed into a transparent tube of equivalent diameter (5 mm) made of PVC. The tube slightly compresses the mixers which avoids radial rotations. Consecutive static mixers are rotated by an angle of 90° each with respect to the previous one. No space is allowed between the mixers. A piece of copper

pipe is inserted in the pipe after the last static mixer in order to stick it and to avoid any axial displacement of the mixers in the pipe.

The continuous and the dispersed phases are stored in separate feed tanks placed on electronic scales to measure their flow rates precisely during the experiment. These flow rates are used to calculate the volume fraction of the dispersed phase:

$$\Phi_d = 100 \frac{Q_d}{(Q_d+Q_c)} \quad (1)$$

Where Q_d and Q_c represent the volume flow rates ($m^3\ s^{-1}$) of the dispersed and continuous phases respectively. The fluids are pumped using two MCP-Z Ismatec® gear pumps equipped with Micropump® magnetically driven heads.

The phases enter in contact in the pipe thanks to a T-junction with a ϒ's form (cf. Figure 2) placed before the static mixers, which introduces the oil phase into the flowing continuous phase. This represents the first step of the emulsification process. Similar online pre-mixing strategies were used by (Hirschberg et al., 2009; Theron et al., 2010). Theron et al. (Theron et al., 2010) chose to inject the dispersed phase perpendicularly to the flowing continuous phase just before the first static mixer while Hirschberg et al. (Hirschberg et al., 2009) introduced the dispersed phase in parallel of the continuous phase directly on the first static mixer. Note that some authors first realise a pre-emulsion using another device (Hoevekamp, 2002; van der Zwan et al., 2008), but in this case, one should be careful to the pumping effects on the pre-emulsion size due to the generated shear and possible breakup, that should be checked at the inlet for each experiment. Baumann et al. (Baumann et al., 2012) indicated that online pre-mixing gives similar drop sizes as off-line pre-mixing but higher standard deviations.

A pressure gauge (0-6 bar, ± 3 mbar) placed at the inlet of static mixers (between the T and the mixers) measures the differential pressure. The static mixers outlet pressure corresponds to the atmospheric pressure. An online Turbiscan (from Formulaction®/France) is placed at the outlet of the static mixers tube to monitor the backscattering signal. A collecting vessel is placed after the

Turbiscan. A sample of each experiment is also withdrawn at the outlet to measure the drop size distribution at-line with a video back lighting probe EZ Probe-D25-L1300 (Becker et al., 2011) after eventual dilution with the continuous phase depending on the dispersed phase fraction. Indeed, the image treatment is limited to about 10%vol. dispersed phase fraction for the considered drop size.

2.4 Emulsification procedure

Emulsifications were performed at room temperature. The dispersed phase was put on the scale without any additives. The continuous phase was also put on a scale, and consisted of distilled water in which the surfactant was dissolved.

The surfactant (Montanox 20) hydrophilic-lipophylic balance (HLB) is 16.7, which is large enough to form direct O/W emulsion when dissolved in the aqueous phase. Its critical micellar concentration (CMC), and therefore saturation concentration at 21°C in pure water, is 8.04×10^{-5} mol L^{-1}. In order to ensure an excess of surfactant, two Montanox 20 concentrations that are higher than the CMC were prepared: 10 g L^{-1} (1%wt., or 8.15×10^{-3} mol L^{-1}) and 25 g L^{-1} (2.5 %wt., or 2.037×10^{-2} mol L^{-1}). According to Becker et al. (Becker et al., 2014), the interfacial tension of silicon oil-water containing between 0.5 to 3.0%wt. of surfactant does not vary significantly. The surfactant has a polar head surface of about 120 Å (Rosen and Kunjappu, 2012). Using this value, the surface coverage of droplets by the surfactant was calculated to be much higher than 100% for all experiments.

The volume fraction of the dispersed phase was varied from 5 to 60%vol., which is close to the theoretical value of phase inversion (Brochette, 1999). Experiments with higher volume fraction of the dispersed phase (75%vol.) were investigated but phase inversion of the samples was observed with naked eyes. As mentioned above, three different silicon oils, with different

viscosities and densities, were used (cf. Table 1). The number of SMX+ static mixers was varied from 1 to 15. The total flow rate was varied between 120 and 1627 mL min^{-1}.

For each experiment, care was taken to achieve steady state conditions, reflected by a constant backscattering signal using the Turbiscan. Typically, steady state in transitional or turbulent flow regimes was achieved very quickly, after 2 minutes.

3. THEORETICAL ASPECTS

Different correlations have been proposed in the literature under equilibrium for both the pressure drop, which determines the energy requirements, and the droplet size determining the product quality, stability and eventual kinetics.

3.1 Flow characteristics

The pressure drop (ΔP) caused by friction between the fluid and the surfaces is useful to predict the energy characteristics of the flow. Correlations for Newtonian single phase fluids in porous media are present for laminar (Liu et al., 2006) and turbulent regimes (Cybulski and Werner, 1986; Pahl and Muschelknautz, 1980; Streiff et al., 1999), as well as for non-Newtonian fluids (Li et al., 1997, 1996; Shah and Kale, 1991). For turbulent flow in a pipe, the pressure drop is described by dimensionless ratio of resistance to inertial forces using Newton number (Ne) and the Reynolds number (Re) as the ratio of inertial to viscous forces:

$$\mathrm{Ne} = 2f_F = \frac{\Delta P}{\rho u_s^2}\frac{D}{L} \quad (2)$$

$$\mathrm{Re} = \frac{\rho u_s D}{\mu} \quad (3)$$

Where f_F represents the friction factor (-), ΔP is the pressure drop (Pa), D is the tube diameter (m) and L its length (m), ρ is the apparent fluid density (kg m^{-3}), μ is the apparent fluid viscosity (Pa s), and u_s is the superficial velocity (m s^{-1}) defined by:

$$u_s = \frac{4Q}{\pi D^2} \quad (4)$$

Where Q is the volume flow rate of the fluid ($m^3\ s^{-1}$).

For pipelines containing mixer elements, pressure drop is usually assumed as uniformly distributed along the pipeline. Therefore, similar correlations were developed for single phase turbulent flow in static mixers, while accounting for the global porosity (φ) of the pipes containing static mixers (Cavatorta et al., 1999; Couvert et al., 2002; Morancais et al., 1999; Pahl and Muschelknautz, 1980; Shah and Kale, 1991; Streiff, 2003; Streiff et al., 1999, 1997; Tallmadge, 1970; Thakur et al., 2003; Theron et al., 2010). This allows comparison between differently structured mixers.

The superficial velocity (u_s, expressed in $m\ s^{-1}$), i.e. in an empty tube, is hence replaced by the interstitial velocity (u_i, in $m\ s^{-1}$) according to:

$$u_i = \frac{u_s}{\varphi} \quad (5)$$

And the pipe diameter (D, m) is replaced by the hydraulic diameter of the pipe (D_h, m):

$$D_h = \frac{4\varphi}{a_g} \quad (6)$$

Where a_g is the mixer specific surface area ($m^2\ m^{-3}$) (Streiff et al., 1999). In this case, the hydraulic Newton number (Ne_h, dimensionless) for a circular pipe containing mixers becomes (Etchells and Meyer, 2003):

$$Ne_h = \frac{\Delta P\ \varphi^2}{\rho\ u_s^2} \frac{D_h}{L} \quad (7)$$

And the hydraulic Reynold number (Re_h, dimensionless) is given by:

$$Re_h = \frac{\rho\ u_s D_h}{\varphi \mu} \quad (8)$$

In two phase fluids, the apparent viscosity of the emulsion is defined by (Taylor, 1932):

$$\mu = \mu_c \left[1 + 2.5\, \Phi_d \left(\frac{\mu_d + {}^2/_5\, \mu_c}{\mu_c + \mu_d}\right)\right] \quad (9)$$

And the apparent fluid density of the emulsion is defined according to (Legrand et al., 2001):

$$\rho = \Phi_d\, \rho_d + (1 - \Phi_d)\rho_c \quad (10)$$

Where ρ_d and ρ_c (kg m^{-3}) are the densities of the dispersed phase and the continuous phase respectively while μ_c and μ_d (Pa s) are the dynamic viscosities of the dispersed phase and the continuous phase respectively (cf. Table 1).

In this work, the interstitial velocity in a pipe containing the mixers varies from $u_i = 0.13 - 1.82$ m s^{-1} (i.e. $u_s = 0.10 - 1.38$ m s^{-1} in an empty pipe), which gives a hydraulic Reynolds number ranging between $Re_h = 160 - 1000$ (i.e. $Re = 425 - 2642$). According to Theron and Sauze (Theron and Sauze, 2011), the turbulent regime in SMX+ mixers is achieved when $Re > 710$ (i.e. $Re_h > 260$, with the porosity considered in this work).

3.2 Correlations for the drop size in turbulent flow

Based on the theory of Kolmogorov (1949) and Hinze (1955), drop breakup is caused by large shear and pressure gradients associated with eddies generated in turbulent flow field. In this theory, breakup takes place either at the turbulent-inertial sub-range (i.e. drops are larger than the smallest eddies, where inertial stresses act on the drop surfaces) or turbulent-viscous dissipation sub-range (i.e. drops are smaller than the smallest eddies, where viscous stresses act on the drop surfaces). The size of smallest eddies is proportional to the Kolmogorov length scale (λ_K) (m), defined by:

$$\lambda_K = \left(\frac{\mu^3}{\rho^3 \epsilon}\right)^{1/4} \quad (11)$$

Where ϵ is the average rate of energy dissipation per unit mass of fluid (W kg^{-1}), expressed by (Ghanem et al., 2014):

$$\epsilon = \frac{\Delta p\, u_s}{\rho_c\, L\varphi} \tag{12}$$

In this work, λ_K varies from 2 to 10μm, and is therefore smaller than the drop size in all experiments which corresponds to the turbulent-inertial sub-range.

Static mixers redistribute the fluid in the radial and tangential directions (transverse to the main flow) using the pumping energy of the flowing fluid which causes distributive mixing by convection. Therefore, they can play the role of promoters of turbulence formation leading to an increase in the energy of eddies, shear and pressure gradients locally, therefore causing drop breakup.

Assuming isotropic flow field and uniform shear and pressure gradients, it is possible to use Kolmogorov-Hinze theory and relate the drop size to the power input and interfacial tension (σ) between the dispersed phase and continuous phase (see (Legrand et al., 2001; Streiff et al., 1997; Theron et al., 2010) for SMX and (Hirschberg et al., 2009) for SMX+). Most correlations assume drop size equilibrium (equal breakup and coalescence rates), except those explicitly accounting for the number of static mixers (n_e).

According to the Kolmogorov-Hinze theory, the maximum diameter of stable drops (d_{max}) in the turbulent-inertial regime is given by (Baumann et al., 2012):

$$d_{max} = C_1 \left(\frac{\sigma}{\rho_c}\right)^{0.6} \epsilon^{-0.4} \tag{13}$$

Where C_1 is a tuning parameter and σ is the interfacial tension (N m^{-1}).

Thereafter, different correlations were proposed using several process parameters as driving force for drop breakup (e.g. We_h, Ne_h, Re_h, ϵ, u_s, number of static mixers) and accounting for different fluid properties (dispersed phase fraction, viscosity ratio, density ratio).

Streiff (Streiff et al., 1997) introduced to Eq. 13 the effect of density ratios between the continuous and dispersed phase $\left(\frac{\rho_c}{\rho_d}\right)$ based on the energy dissipation as driving force for breakup in SMX mixers:

$$d = C_2 \left(\frac{\sigma}{\rho_c}\right)^{0.6} \left(\frac{\rho_c}{\rho_d}\right)^{0.1} \epsilon^{-0.4} \tag{14}$$

Middleman (Middleman, 1974) adapted Eq. 13 of Kolmogorov-Hinze for Kenics static mixers using as driving forces for drop breakup the hydraulic Newton number (Eq. 7) and the hydraulic Weber number (We_h, ratio of inertial to interfacial forces, Eq.16), but both correlations may be considered equivalent if the energy dissipation is assumed to be given by Eq.12:

$$\frac{d_{max}}{D_h} = C_1 \, We_h^{-0.6} Ne_h^{-0.4} \tag{15}$$

$$We_h = \frac{\rho_c u_s^2 D_h}{\varphi^2 \sigma} \tag{16}$$

Assuming $Ne_h \propto Re_h^{-0.25}$ (Blasius law), Eq. 15 is reduced to:

$$\frac{d_{max}}{D_h} = C_3 \, We_h^{-0.6} Re_h^{0.1} \tag{17}$$

The volume fraction of the dispersed phased (Φ_d) was accounted for using hydraulic Weber number alone as a driving force for drop breakup, (Poux and Canselier, 2004), which added a second tuning parameter:

$$\frac{d_{32}}{D_h} = C_4 \, s(1 + C_5 \, \Phi_d) We^{-3/5} \tag{18}$$

Calabrese et al. (Calabrese et al., 1986) and Davies (Davies, 1985) introduced the effect of the ratio of the viscosity of the dispersed phase to the continuous phase to the Middleman equation (Eq. 15):

$$\frac{d_{max}}{D_h} = C_6 \left(1 + C_7 \left(\frac{\mu_d}{\mu_c}\right) \left(\frac{d}{D_h}\right)^{1/3} \frac{We_h \, Ne_h^{1/3}}{Re_h}\right)^{0.6} We_h^{-0.6} Ne_h^{-0.4} \tag{19}$$

The combined effect of dispersed phased fraction and density ratio was accounted for by Streiff et al. (Streiff et al., 1997) based on the drop breakup driving forces of energy dissipation and interstitial velocity:

$$d = C_8 (1 + C_9 \Phi_d) \left(\frac{(1+ C_{10} u_i)We_c}{2}\right)^{0.6} \left(\frac{\sigma}{\rho_c}\right)^{0.6} \left(\frac{\rho_c}{\rho_d}\right)^{0.1} \epsilon^{-0.4} \quad (20)$$

Where We_c is the critical Weber number (-). Note that this equation has three tuning parameters.

The superficial velocity was also directly considered as a driving force for breakup (Barega et al., 2013):

$$\frac{d_{32}}{D} = (1 + C_{11} \Phi_d) \left(\frac{\rho u_s^2 D}{\sigma}\right)^{\alpha(\Phi_d)} \left(\frac{\rho u_s D}{\mu_c}\right)^{\beta(\Phi_d)} \left(\frac{\mu_d}{\mu_c}\right)^{\gamma} \quad (21)$$

Where α, β, γ and C_{11} are tuning parameters.

Theron et al. (Theron et al., 2010), as Maa and Hsu before (Maa and Hsu, 1996), introduced the number of SMX static mixer elements (n_e) in Middleman equation as follows:

$$\frac{d_{32}}{D} = C_{12} We^{-0.6} Re^{0.1} n_e^{-0.2} \quad (22)$$

The mean diameters, d_{32} (i.e. the Sauter mean diameter) and d_{43}, can be calculated using the drop size distribution in number, n(d) (Middleman, 1974):

$$d_{ab} = \left(\frac{\sum_{i=1}^{n} n_i d_i^a}{\sum_{i=1}^{n} n_i d_i^b}\right)^{\left(\frac{1}{a-b}\right)} \quad (23)$$

As the objective of this work is to develop a correlation that describes the drop size for flow regimes going from transitional to turbulent, for low and high Reynolds numbers, then the approximation of Blasius will not be used, as the Reynolds and Newton numbers may not be correlated. The proposed correlation should thus be based on either the energy dissipation or Newton number. Moreover, it is aimed to take into account the number of static mixers in the correlation.

4. RESULTS AND DISCUSSION

The evolution of the droplets diameter and the droplets size distribution in static mixer processes is governed by physicochemical parameters (such as the viscosity and density ratios, the surfactant dynamics and efficiency), concentrations (fraction of the dispersed phase, surfactant), and hydrodynamic parameters. These latter are affected by the flow rate and the geometrical parameters (mixer diameter, length, porosity and structure).

The influence of key parameters was investigated as follows: a process configuration was selected, i.e. a number of SMX+ static mixers and a series of oil-in-water emulsion experiments were performed for each oil viscosity according to the protocol detailed in the materials and method section. For each series of experiments, the Reynolds number and the volume fraction of the dispersed phase were varied randomly to avoid any memory effect of one experiment on the following one. At the end of the series, the first experiment was repeated to validate the whole series. And between each series, the experimental setup was abundantly rinsed with distilled water.

4.1 Droplet size distribution measurement

The droplet size distribution was measured at-line by the video probe for all experiments. This measurement technique was widely used for emulsion size characterisation (Becker et al., 2014). It has the advantage of working online for diluted emulsions, up to 10%vol. As the volume fraction in this work is increased up to 60%vol., a sample is withdrawn, diluted 10 times, e.g. 10mL of sample is diluted in a 100mL volumetric flask with the continuous phase, and measured using the video probe under gentle mixing (at-line). The attainment of reproducible results is indeed an essential pre-requisite for any emulsification experiment with a volume fraction of the dispersed phase higher than 10%vol.

Turbiscan was used for backscattering measurement online in order to detect equilibrium in drop size (equal breakup and coalescence). Note that backscattering measurements may be used to predict the mean drop size after three-dimensional calibration (as a function of the volume fraction of the dispersed phase, drop size and refractive index), which quickly becomes time-consuming. Moreover, this would only give the mean diameter and not the drop size distribution.

Figure 3 shows the cumulative size distributions measured using the video probe with varying operating conditions. It can be seen that the reproducibility of the experiments is good regardless the volume fraction, viscosity or Reynolds number. The dilution of the sample for video probe measurements can also be assumed not to influence the measurement of the drop size distribution.

4.2 Influence of the number of SMX+ mixers elements

The influence of the geometrical parameter is studied by varying the number of SMX+ in the pipe from 1 to 15.

Figure 4 a) shows the effect of the number of SMX+ static mixers on d_{32} for different oil fractions (using V20 Silicon oil) and Figure 4 b) for different silicon oil viscosities (using Φ_d = 20%vol). The results were obtained with a hydraulic energy dissipation of about 1000W kg^{-1}. Both figures show that increasing the number of SMX+ static mixers in the pipe allows decreasing the drop size. This is due to the increase in the residence time and therefore dispersion kinetics. Figure 4 a) shows that regardless the volume fraction of the dispersed phase; the drop size reaches an equilibrium value after 5 SMX+ which means that the breakup is importantly reduced after the 5^{th} mixer (equilibrium between breakup and coalescence). This indicates that the first five SMX+ are mainly efficient for breakup, and the following mixers will be responsible for an increase in the pressure drop, which has to be avoided. By the same way, much more breakup takes place between the 1^{st} and 3^{rd} mixer than between the 3^{rd} and 5^{th} one. In this work,

we will be interested in modelling the part of this curve where drop size evolves. It can be seen on Figure 4 a) that the oil volume fraction has a negligible effect on the drop size.

Figure 4 b) also shows that the increase of the number of SMX+ induces a decrease in the drop size with the V20 silicon oil. Here again, the drop size reaches an equilibrium value after 5 SMX+ confirming the result presented above. However, it has to be noted that surprisingly the increase of the oil viscosity is responsible of a decrease of the drop size. This effect is more pronounced when the oil viscosity is increased from 20 to 100 mPa s; while the effect is non-existent when the increase of the oil viscosity is from 100 to 350 mPa s. Note that these experiments were realized with 20%vol dispersed phased fraction. These experiments were repeated for the different oil concentrations. At low oil fractions, the tendency was previously found to be almost opposite (Becker et al., 2011), and so in accordance to the literature (Baumann et al., 2012). This reveals a combined effect of concentration and viscosity.

4.3 Influence of the hydrodynamic parameter

The influence of the hydrodynamic parameter on the drop size is investigated by changing the total input flow rate, leading to different energy dissipation levels. The volume fractions of 20%vol., 35%vol., 50%vol. and 60%vol. of the dispersed phase with a V20 viscosity are considered in these series of experiments. The number of SMX+ static mixers is fixed at 10-11 in order to ensure a constant drop size.

Figure 5 a) shows the effect of the energy dissipation on d_{32} for different dispersed phase fractions while Figure 5 b) shows the effect of the energy dissipation on d_{32} for different oil viscosities. In accordance with the literature (Barega et al., 2013; Das et al., 2013; Theron et al., 2010), both figures show that increasing ϵ (or the velocity or the Reynolds number) induces a slight decrease in d_{32} due to the increase in the level of turbulence involving higher inertial forces and pressure gradients. However, d_{32} is constant above hydraulic ϵ= 1000 W kg^{-1}, which could be explained by a balance between breakup and coalescence mechanisms. The effects of the

dispersed phase fraction or viscosity are found to be negligible in front of that of ϵ. Thus, the influence of the energy dissipation is to be of first order compared to the volume fraction or viscosity of the dispersed phase, as will be confirmed in the next section.

Note that the apparent density and viscosity of the fluid phase, used in the calculation of the energy dissipation rate and the Reynolds number, are quite the same for all the experiments and ranged respectively between 958 to 998 kg m^{-3} and 1.015 to 3.158 mPa s respectively, while the flow rate varied from 120 to 1627 mL min^{-1}.

4.4 Correlation to predict the Sauter mean diameter (d_{32})

This part of the study intends to propose a new form of the Middleman correlation which considers the flow properties through the hydraulic Newton number and properties of the droplets surface through the hydraulic Weber number. The correlation is aimed to be able to forecast the drop size evolution until a constant size is reached. Thus, the influence of the number of SMX+ static mixer (n_e) (equivalent to a residence time) is added to these two dimensionless numbers. As reported above, the experimental results highlighted that the influence of the viscosity is of the second order and the influence of the volume fraction of the dispersed phase is negligible on the range studied; while the influence of the number of SMX+ and the Reynolds number are of first order. Hence, the influence of the viscosity ratio and the volume fraction of the dispersed phase are lumped into the tuning parameter C_1. Note also that it was preferred to use the original correlation of Middleman that uses the hydraulic Newton number, rather than the latter correlations based on the Reynolds number, in order to avoid adding a supplementary assumption that $Ne_h \propto Re_h^{-0.25}$ (Blasius law). Indeed, some of the results are reached in a transitional flow while the other part is achieved in turbulent flow; thus, the linearity relationship between the Reynolds number and the Newton number is not confirmed. Note also that the Middleman correlation constitutes the equivalence of the original Kolmogorov-Hinze correlation proposed

for turbulent systems, for static mixers. The results are presented on Figure 6 and the obtained correlation is:

$$\frac{d_{32}}{D_h} = C_1\, We_h^{-0.6}\, Ne_h^{-0.4}\, n_e^{-C_2} = \frac{1}{D_h} C_1 \left(\frac{\sigma}{\rho_c}\right)^{0.6} \epsilon^{-0.4}\, n_e^{-C_2} \qquad (24)$$

The correlation was established by using experimental results obtained with 1 to 5 SMX+ , according to the results presented above which highlighted that only the first five SMX+ are efficient to breakup. A volume fraction of the dispersed phase ranging from 5 to 60%vol. was considered, and the three silicon oil viscosities (20, 100 and 350 mPa s) were considered. Finally, the hydraulic Newton number was varied between 5 and 130, corresponding to a hydraulic Reynolds number ranging from 220 to 950. Thus, the correlation is usable both in the transitional and turbulent flow regimes.

Figure 6 shows the modelling results. The values of the parameters, obtained by linear regression, are $C_1 = 1.7$ and $C_2 = 0.27$. Only the experiments done at low energy dissipation are not caught by the model. This is due to the fact that at low energy dissipation, the drop size distribution is very wide. Therefore, the calculation of d_{32} might be disturbed by the presence of small number of big drops detected by image treatment. Moreover, at very low flow rates, controlling precisely the flow rates and therefore the volume fraction of oil is more difficult with the used pumps. It has to be noted that the exponent values of the hydraulic Weber number (i.e. -0.6) and the hydraulic Newton number (i.e. -0.4) are the same as those reported in the Middleman correlation (Middleman, 1974). The obtained exponent value of n_e is close to those reported in the literature for other static mixers (Baumann et al., 2012; Theron et al., 2010). Hence, the influence of the static mixers type (SMX, SMX+, Kenics) on the process performances seems to be negligible.

5. CONCLUSIONS

The objective of this study was to push the limit of modelling the emulsification process by new SMX+ static mixers. This kind of static mixers is particularly recommended for viscous liquid-

liquid dispersion causing limited pressure drop. The reported experimental results allow investigating the influence of some physicochemical parameters (the volume fraction of the dispersed phase and its viscosity), the geometric parameter through the number of SMX+ in the pipe and the hydrodynamic parameter (the Reynolds diameter) on the drop size. The comparison was based on the Sauter mean diameter (d_{32}).

The obtained results show that the increase of the energy dissipation rate or the number of SMX+ static mixers induce a decrease in the d_{32} diameter while the increase of the dispersed fraction has a negligible effect and its viscosity seems to have no significant effect when it is higher than 100 mPa s. More importantly, the decrease in the d_{32} with the increase of the number of SMX+ is mainly limited to the first five SMX+, whatever the value of the energy dissipation rate (or the Newton number or the Reynolds number), in the studied range. In fact, the following SMX+ static mixer added after the five first ones will only increase the pressure drop but will not have any influence on the d_{32}. Hence, it clearly appears that the influence of the energy dissipation rate and the number of the SMX+ static mixer are of the same order of magnitude whereas the influence of the volume fraction of the dispersed phase and its viscosity are lower.

Finally, a correlation of type Middleman was established. This one takes into consideration the number of SMX+ mixer elements. The correlation is adapted to situations where the drop size distribution is not yet fully established. The exponents of each parameter of the correlation confirmed that the number of SMX+ has almost the same influence on the d_{32} as the Newton number.

SYMBOLS

a_g : Specific diameter ($m^2\ m^{-3}$)

D : Pipe diameter (m)

d : Drop diameter (µm)

d_{32} : Sauter mean diameter (µm)

d_{max} : Maximum diameter of stable drops (µm)

D_h : Hydraulic pipe diameter (m)

DSD : Drop size distribution

f_F : Friction factor (-)

L : Length (m)

Ne : Newton number (-)

Ne_h : Hydraulic Newton number (-)

n_e : Number of SMX+ in the pipe (-)

Q : Volume flow rate ($m^3\ s^{-1}$)

Q_d : Volume flow rate of the dispersed phase ($m^3\ s^{-1}$)

Q_c : Volume flow rate of the continuous phase ($m^3\ s^{-1}$)

Re : Reynolds number (-)

Re_h : Hydraulic Reynolds number (-)

u_i : Interstitial velocity ($m\ s^{-1}$)

u_s : Superficial velocity ($m\ s^{-1}$)

We : Weber number (-)

We_h : Hydraulic Weber number (-)

Greek symbols

ΔP : Pressure Drop (Pa)

ε : Porosity, i.e. void fraction of the static mixer (-)

ϵ : Energy dissipation rate (W kg^{-1})

φ : Global porosity (%)

Φ_d : Volume fraction of the dispersed phase (%vol.)

λ_K : Kolmogorov length scale (m)

μ : Apparent dynamic viscosity of the emulsion (Pa s)

μ_d : Dynamic viscosity of the dispersed phase (Pa s)

μ_c : Dynamic viscosity of the continuous phase (Pa s)

ρ : Apparent density of the emulsion (kg m^{-3})

ρ_d : Density of the dispersed phase (kg m^{-3})

ρ_c : Density of the continuous phase (kg m^{-3})

σ : Interfacial tension (N m^{-1})

ACKNOWLEDGEMENTS

The authors would gratefully thank Alain RIVOIRE, Jean-Marc GALVAN and Julian BECKER, for their help in the field of *in situ* video monitoring and image treatment, Mathilde ESCHMANN and François WARRICK for their experimental work.

REFERENCES

Al Taweel, A.M., Li, C., Gomaa, H.G., Yuet, P., 2007. Intensifying Mass Transfer Between Immiscible Liquids: Using Screen-type Static Mixers. Chem. Eng. Res. Des. 85, 760–765. doi:10.1205/cherd06180

Anxionnaz, Z., Cabassud, M., Gourdon, C., Tochon, P., 2008. Heat exchanger/reactors (HEX reactors): Concepts, technologies: State-of-the-art. Chem. Eng. Process. Process Intensif. 47, 2029–2050. doi:10.1016/j.cep.2008.06.012

Barega, E.W., Zondervan, E., Haan, A.B. de, 2013. Influence of Physical Properties and Process Conditions on Entrainment Behavior in a Static-Mixer Settler Setup. Ind. Eng. Chem. Res. 52, 2958–2968. doi:10.1021/ie301580m

Baumann, A., Jeelani, S.A.K., Holenstein, B., Stössel, P., Windhab, E.J., 2012. Flow regimes and drop break-up in SMX and packed bed static mixers. Chem. Eng. Sci. 73, 354–365. doi:10.1016/j.ces.2012.02.006

Bayat, M., Rahimpour, M.R., Taheri, M., Pashaei, M., Sharifzadeh, S., 2012. A comparative study of two different configurations for exothermic–endothermic heat exchanger reactor. Chem. Eng. Process. Process Intensif. 52, 63–73. doi:10.1016/j.cep.2011.11.010

Becker, P.J., Puel, F., Chevalier, Y., Sheibat-Othman, N., 2014. Monitoring silicone oil droplets during emulsification in stirred vessel: Effect of dispersed phase concentration and viscosity. Can. J. Chem. Eng. 92, 296–306. doi:10.1002/cjce.21885

Becker, P.J., Puel, F., Henry, R., Sheibat-Othman, N., 2011. Investigation of Discrete Population Balance Models and Breakage Kernels for Dilute Emulsification Systems. Ind. Eng. Chem. Res. 50, 11358–11374. doi:10.1021/ie2006033

Berkman, P.D., Calabrese, R.V., 1988. Dispersion of viscous liquids by turbulent flow in a static mixer. AIChE J. 34, 602–609. doi:10.1002/aic.690340409

Brochette, P., 1999. Émulsification - Élaboration et étude des émulsions. Tech. Ing.

Calabrese, R.V., Chang, T.P.K., Dang, P.T., 1986. Drop breakup in turbulent stirred-tank contactors. Part I: Effect of dispersed-phase viscosity. AIChE J. 32, 657–666. doi:10.1002/aic.690320416

Cavatorta, O.N., Böhm, U., de del Giorgio, A.M.C., 1999. Fluid-dynamic and mass-transfer behavior of static mixers and regular packings. AIChE J. 45, 938–948. doi:10.1002/aic.690450504

Chen, S.J., Libby, D.R., 1978. Gas-liquid and liquid-liquid dispersions in a Kenics mixer. Presented at the 71st Annual AIChE Meeting, Houston, Texas, USA, pp. 8–18.

Couvert, A., Péculier, M.-F., Laplanche, A., 2002. Pressure Drop and Mass Transfer Study in Static Mixers with Gas Continuous Phase. Can. J. Chem. Eng. 80, 727–733. doi:10.1002/cjce.5450800426

Couvert, A., Sanchez, C., Charron, I., Laplanche, A., Renner, C., 2006. Static mixers with a gas continuous phase. Chem. Eng. Sci. 61, 3429–3434. doi:10.1016/j.ces.2005.11.040

Cybulski, A., Werner, K., 1986. Static mixers-criteria for applications and selection. Int. Chem. Eng. 26, 171–180.

Das, M.D., Hrymak, A.N., Baird, M.H.I., 2013. Laminar liquid–liquid dispersion in the SMX static mixer. Chem. Eng. Sci. 101, 329–344. doi:10.1016/j.ces.2013.06.047

Das, P.K., Legrand, J., Morançais, P., Carnelle, G., 2005. Drop breakage model in static mixers at low and intermediate Reynolds number. Chem. Eng. Sci. 60, 231–238. doi:10.1016/j.ces.2004.08.003

Davies, J.T., 1985. Drop sizes of emulsions related to turbulent energy dissipation rates. Chem. Eng. Sci. 40, 839–842. doi:10.1016/0009-2509(85)85036-3

Etchells, A.W., Meyer, C.F., 2003. Mixing in Pipelines, in: Handbook of Industrial Mixing: Science and Practice. John Wiley & Sons, pp. 391–477.

Fradette, L., Brocart, B., Tanguy, P.A., 2007. Comparison of Mixing Technologies for the Production of Concentrated Emulsions. Chem. Eng. Res. Des. 85, 1553–1560. doi:10.1205/cherd06015

Ghanem, A., Habchi, C., Lemenand, T., Valle, D.D., Peerhossaini, H., 2014. Mixing performances of swirl flow and corrugated channel reactors. Chem. Eng. Res. Des. 92, 2213–2222. doi:10.1016/j.cherd.2014.01.014

Haas, P.A., 1987. Turbulent dispersion of aqueous drops in organic liquids. AIChE J. 33, 987–995. doi:10.1002/aic.690330611

Hirschberg, S., Koubek, R., F.Moser, Schöck, J., 2009. An improvement of the Sulzer SMX™ static mixer significantly reducing the pressure drop. Chem. Eng. Res. Des., 13th European Conference on Mixing: New developments towards more efficient and sustainable operations 87, 524–532. doi:10.1016/j.cherd.2008.12.021

Hoevekamp, T.B., 2002. Experimental and Numerical Investigation of Porous Media Flow with Regard to the Emulsion Process. Swiss Federal Institute of Technology Zürich, Zürich, Suisse.

Kiss, N., Brenn, G., Pucher, H., Wieser, J., Scheler, S., Jennewein, H., Suzzi, D., Khinast, J., 2011. Formation of O/W emulsions by static mixers for pharmaceutical applications. Chem. Eng. Sci. 66, 5084–5094. doi:10.1016/j.ces.2011.06.065

Laporte, M., Loisel, C., Della Valle, D., Riaublanc, A., Montillet, A., 2014. Flow process conditions to control the void fraction of food foams in static mixers. J. Food Eng. 128, 119–126. doi:10.1016/j.jfoodeng.2013.12.017

Legrand, J., Morançais, P., Carnelle, G., 2001. Liquid-Liquid Dispersion in an SMX-Sulzer Static Mixer. Chem. Eng. Res. Des., 4th International Symposium on Mixing in Industrial Processes 79, 949–956. doi:10.1205/02638760152721497

Leng, D.E., Calabrese, R.V., 2003. Immiscible Liquid–Liquid Systems, in: Paul, E.L., Atiemo-Obeng, V.A., Kresta, S.M. (Eds.), Handbook of Industrial Mixing. John Wiley & Sons, Inc., pp. 639–753.

Li, H.Z., Fasol, C., Choplin, L., 1997. Pressure Drop of Newtonian and Non-Newtonian Fluids Across a Sulzer SMX Static Mixer. Chem. Eng. Res. Des., Fluid Flow 75, 792–796. doi:10.1205/026387697524461

Li, H.Z., Fasol, C., Choplin, L., 1996. Hydrodynamics and heat transfer of rheologically complex fluids in a Sulzer SMX static mixer. Chem. Eng. Sci., Chemical Reaction Engineering: From Fundamentals to Commercial Plants and Products 51, 1947–1955. doi:10.1016/0009-2509(96)00052-8

Liu, S., Hrymak, A.N., Wood, P.E., 2006. Laminar mixing of shear thinning fluids in a SMX static mixer. Chem. Eng. Sci. 61, 1753–1759. doi:10.1016/j.ces.2005.10.026

Liu, S., Hrymak, A.N., Wood, P.E., 2005. Drop Breakup in an SMX Static Mixer in Laminar Flow. Can. J. Chem. Eng. 83, 793–807. doi:10.1002/cjce.5450830501

Lobry, E., Theron, F., Gourdon, C., Le Sauze, N., Xuereb, C., Lasuye, T., 2011. Turbulent liquid–liquid dispersion in SMV static mixer at high dispersed phase concentration. Chem. Eng. Sci. 66, 5762–5774. doi:10.1016/j.ces.2011.06.073

Maa, Y.F., Hsu, C., 1996. Liquid-liquid emulsification by static mixers for use in microencapsulation. J. Microencapsul. 13, 419–433. doi:10.3109/02652049609026028

Meijer, H.E.H., Singh, M.K., Anderson, P.D., 2012. On the performance of static mixers: A quantitative comparison. Prog. Polym. Sci., Topical Issue on Polymer Physics 37, 1333–1349. doi:10.1016/j.progpolymsci.2011.12.004

Middleman, S., 1974. Drop Size Distributions Produced by Turbulent Pipe Flow of Immiscible Fluids through a Static Mixer. Ind. Eng. Chem. Process Des. Dev. 13, 78–83. doi:10.1021/i260049a015

Morancais, P., Hirech, K., Carnelle, G., Legrand, J., 1999. Friction Factor in Static Mixer and Determination of Geometric Parameters of Smx Sulzer Mixers. Chem. Eng. Commun. 171, 77–93. doi:10.1080/00986449908912750

Paglianti, A., Montante, G., 2013. A mechanistic model for pressure drops in corrugated plates static mixers. Chem. Eng. Sci. 97, 376–384. doi:10.1016/j.ces.2013.04.042

Pahl, M., Muschelknautz, E., 1980. Static Mixers and Their Applications. Chem. Ing. Tech. 52, 285–291. doi:10.1002/cite.330520402

Poux, M., Canselier, J.-P., 2004. Procédés d'émulsification - Techniques et appareillage. Tech. Ing.

Rama Rao, N.V., Baird, M.H.I., Hrymak, A.N., Wood, P.E., 2007. Dispersion of high-viscosity liquid–liquid systems by flow through SMX static mixer elements. Chem. Eng. Sci. 62, 6885–6896. doi:10.1016/j.ces.2007.08.070

Rosen, M.J., Kunjappu, J.T., 2012. Surfactants and Interfacial Phenomena. John Wiley & Sons.

Shah, N.F., Kale, D.D., 1991. Pressure drop for laminar flow of non-Newtonian fluids in static mixers. Chem. Eng. Sci. 46, 2159–2161. doi:10.1016/0009-2509(91)80175-X

Streiff, F.A., 2003. Statisches Mischen, in: Kraume, -Ing tthias (Ed.), Mischen und Rühren. Wiley-VCH Verlag GmbH & Co. KGaA, pp. 197–220.

Streiff, F.A., Jaffer, S., Schneider, G., 1999. The design and application of static mixer technology, 3rd ed.

Streiff, F.A., Mathys, P., Fischer, T.U., 1997. New fundamentals for liquid–liquid dispersion using static mixers. Récents Prog. En Génie Procédés 11, 307–314.

Tallmadge, J.A., 1970. Packed bed pressure drop—an extension to higher Reynolds numbers. AIChE J. 16, 1092–1093. doi:10.1002/aic.690160639

Taylor, G.I., 1932. The Viscosity of a Fluid Containing Small Drops of Another Fluid. Proc. R. Soc. Lond. Ser. Contain. Pap. Math. Phys. Character 138, 41–48.

Thakur, R.K., Vial, C., Nigam, K.D.P., Nauman, E.B., Djelveh, G., 2003. Static Mixers in the Process Industries—A Review. Chem. Eng. Res. Des., Reaction Engineering: Microstructured Reactors 81, 787–826. doi:10.1205/026387603322302968

Theron, F., Le Sauze, N., Ricard, A., 2010. Turbulent Liquid−Liquid Dispersion in Sulzer SMX Mixer. Ind. Eng. Chem. Res. 49, 623–632. doi:10.1021/ie900090d

Theron, F., Sauze, N.L., 2011. Comparison between three static mixers for emulsification in turbulent flow. Int. J. Multiph. Flow 37, 488–500. doi:10.1016/j.ijmultiphaseflow.2011.01.004

van der Zwan, E.A., Schroën, C.G.P.H., Boom, R.M., 2008. Premix membrane emulsification by using a packed layer of glass beads. AIChE J. 54, 2190–2197. doi:10.1002/aic.11508

Van Gerven, T., Stankiewicz, A., 2009. Structure, Energy, Synergy, Time—The Fundamentals of Process Intensification. Ind. Eng. Chem. Res. 48, 2465–2474. doi:10.1021/ie801501y

Yamamoto, T., Kawasaki, H., Kumazawa, H., 2007. Relationship between the Dispersed Droplet Diameter and the Mean Power Input for Emulsification in Three Different Types of Motionless Mixers. J. Chem. Eng. Jpn. 40, 673–678. doi:10.1252/jcej.40.673

Figure captions:

Figure 1: Pictures of SMX+ static mixer used.

Figure 2: Schematic diagram of the experimental set-up.

Figure 3: Examples of cumulative drop size protocol validation on emulsification process. Results are carried out with 5 SMX+ static mixers in the pipe.

Figure 4: Influence of the number of SMX+ mixers: a) Effect of numbers of SMX+ (V20, Energy dissipation rate = 5000 W kg^{-1}); b) Effect of numbers of SMX+ (ϕ_d = 20%vol., Energy dissipation rate = 3000 W kg^{-1}).

Figure 5: Influence of the hydrodynamic parameters: a) Effect of the volume fraction of the dispersed phase (V20, 10 SMX+); b) Effect of the viscosity on d_{32} (ϕ_d = 10%vol., 10 SMX+).

Figure 6: Middleman type correlation for the experimental data in terms of Weber number, Reynolds number, SMX+ static mixers number and viscosity ratio.

Figure 1

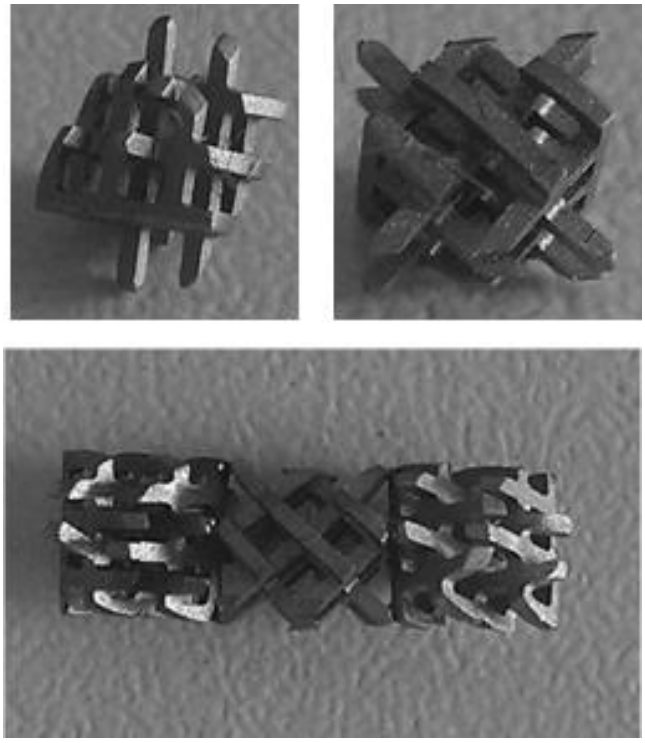

Figure 2

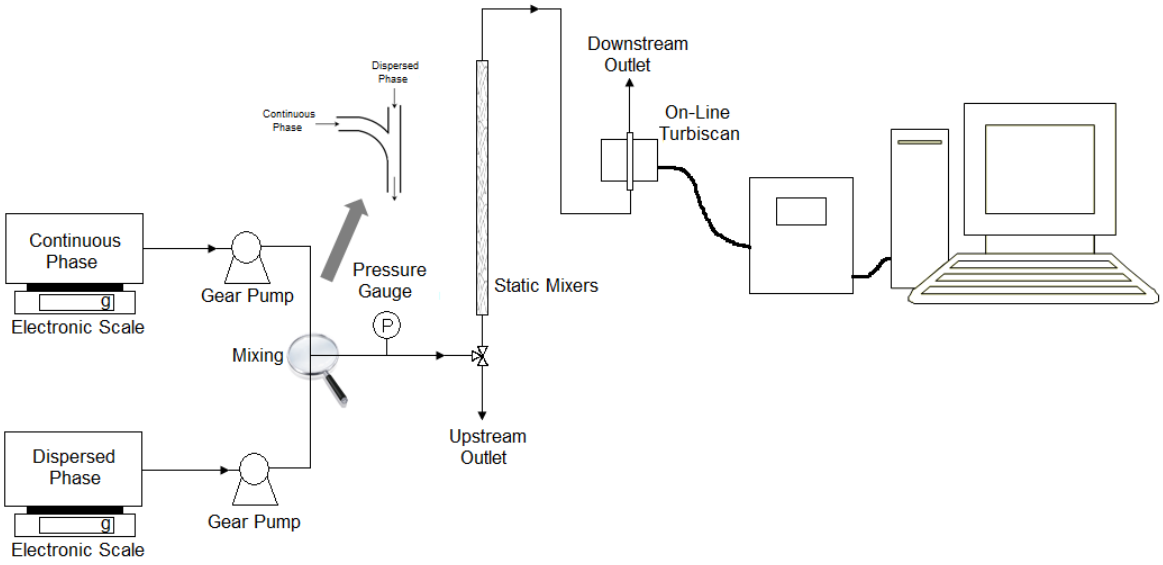
Dispersed Phase
Continuous Phase
Downstream Outlet
On-Line Turbiscan
Continuous Phase
Gear Pump
Pressure Gauge
Static Mixers
Electronic Scale
P
Mixing
Upstream Outlet
Dispersed Phase
Gear Pump
Electronic Scale

Figure 3

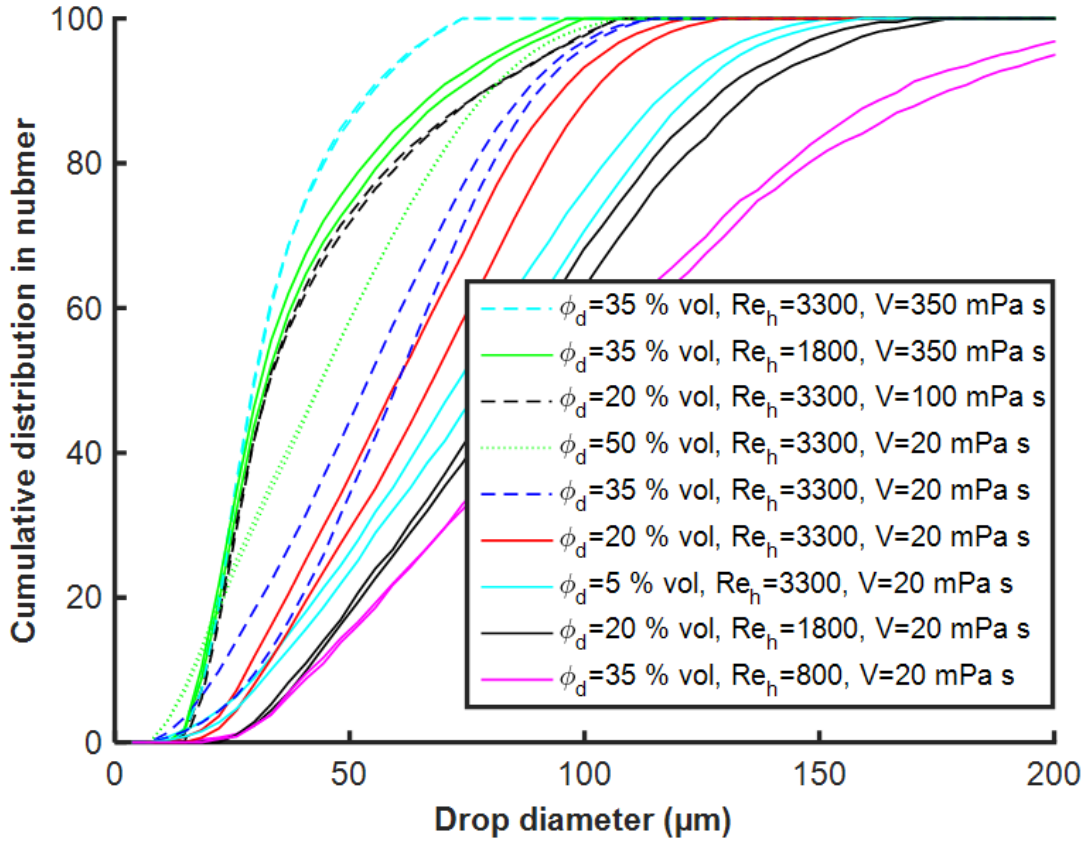
Cumulative distribution in nubmer
Drop diameter (μm)
0
20
40
60
80
100
0
50
100
150
200
ϕ_d=35 % vol, Re_h=3300, V=350 mPa s
ϕ_d=35 % vol, Re_h=1800, V=350 mPa s
ϕ_d=20 % vol, Re_h=3300, V=100 mPa s
ϕ_d=50 % vol, Re_h=3300, V=20 mPa s
ϕ_d=35 % vol, Re_h=3300, V=20 mPa s
ϕ_d=20 % vol, Re_h=3300, V=20 mPa s
ϕ_d=5 % vol, Re_h=3300, V=20 mPa s
ϕ_d=20 % vol, Re_h=1800, V=20 mPa s
ϕ_d=35 % vol, Re_h=800, V=20 mPa s

Figure 4

(a)

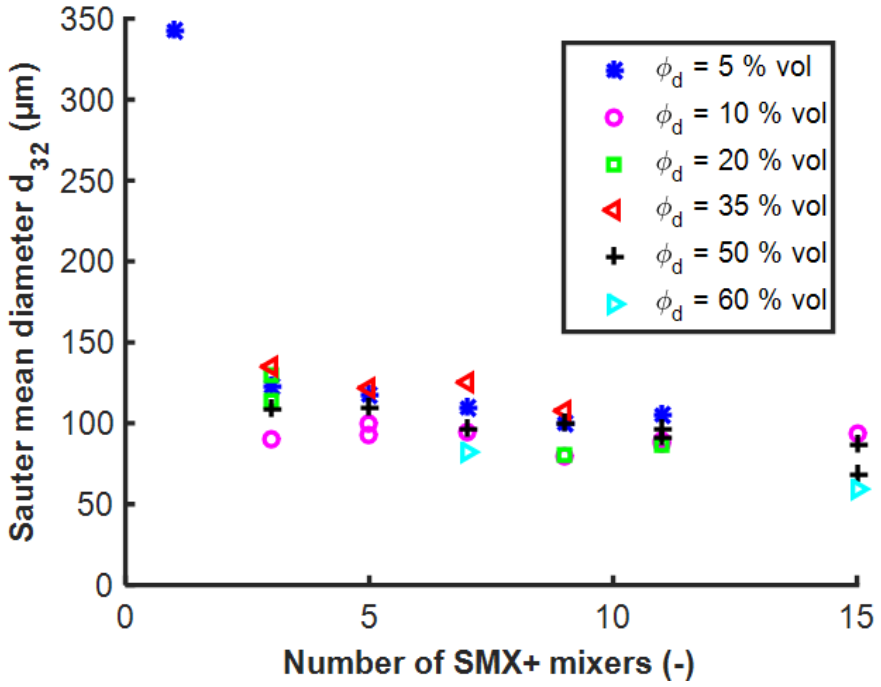
Sauter mean diameter d_{32} (µm)
Number of SMX+ mixers (-)
ϕ_d = 5 % vol
ϕ_d = 10 % vol
ϕ_d = 20 % vol
ϕ_d = 35 % vol
ϕ_d = 50 % vol
ϕ_d = 60 % vol
0
50
100
150
200
250
300
350
0
5
10
15

(b)

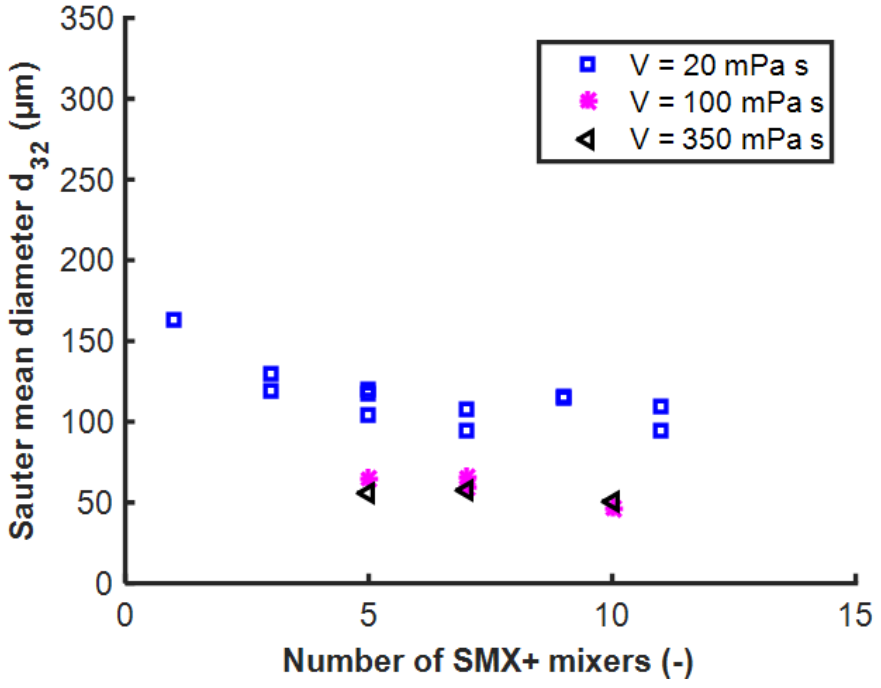
Sauter mean diameter d_{32} (µm)
Number of SMX+ mixers (-)
V = 20 mPa s
V = 100 mPa s
V = 350 mPa s
0
50
100
150
200
250
300
350
0
5
10
15

Figure 5

(a)

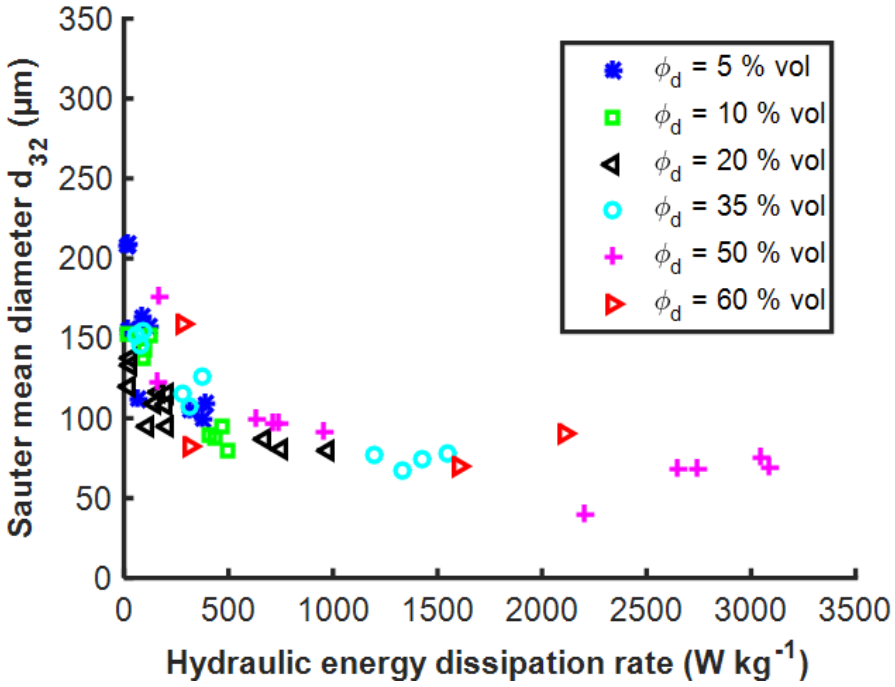
Sauter mean diameter d32 (µm)
Hydraulic energy dissipation rate (W kg-1)
ϕd = 5 % vol
ϕd = 10 % vol
ϕd = 20 % vol
ϕd = 35 % vol
ϕd = 50 % vol
ϕd = 60 % vol
0
50
100
150
200
250
300
350
0
500
1000
1500
2000
2500
3000
3500

(b)

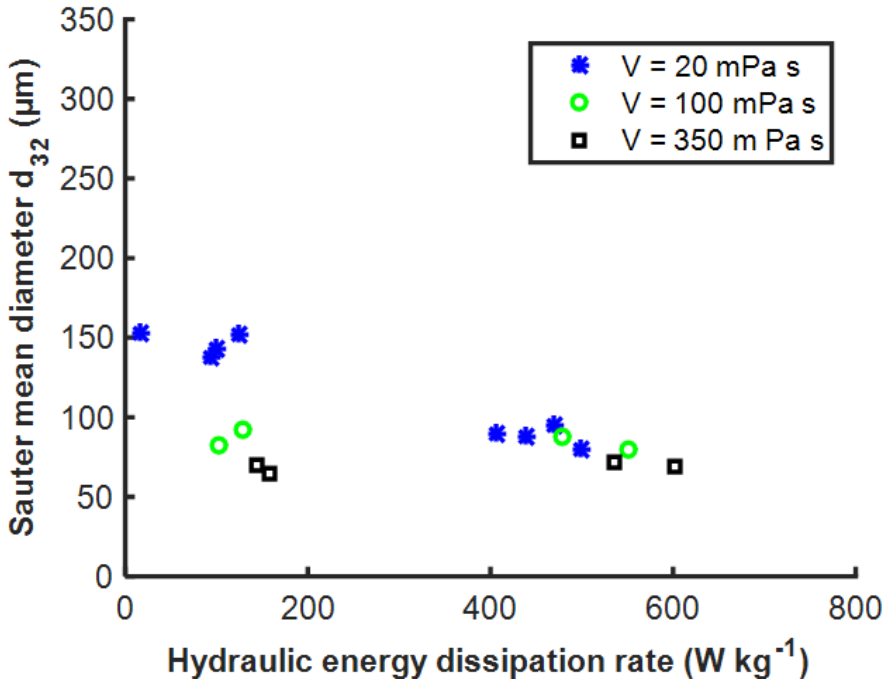
Sauter mean diameter d32 (µm)
Hydraulic energy dissipation rate (W kg-1)
V = 20 mPa s
V = 100 mPa s
V = 350 m Pa s
0
50
100
150
200
250
300
350
0
200
400
600
800

Figure 6

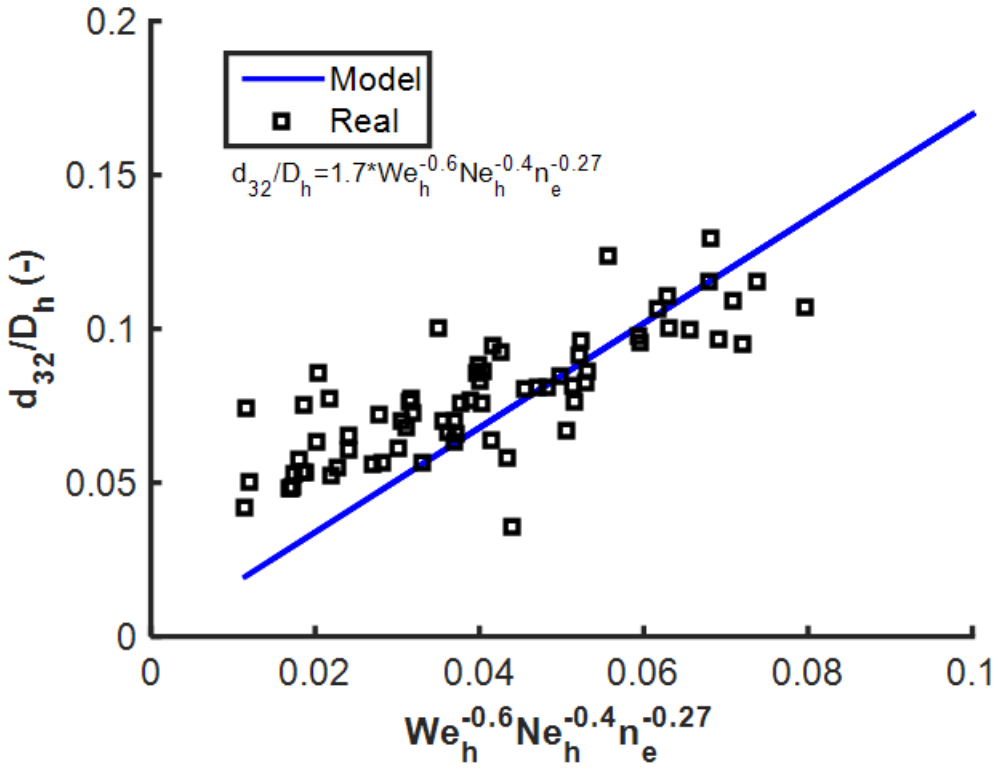
Model
Real
$d_{32}/D_h=1.7*We_h^{-0.6}Ne_h^{-0.4}n_e^{-0.27}$
d_{32}/D_h (-)
$We_h^{-0.6}Ne_h^{-0.4}n_e^{-0.27}$
0
0.05
0.1
0.15
0.2
0.02
0.04
0.06
0.08

Table 1

Physico-Chemical properties of silicon oil in distilled water emulsion stabilized using Montanox 20, at 20°C

Properties	**Silicon Oil**		
	V20	**V100**	**V350**
Dispersed phase density ρ_d (kg m^{-3})	948.8	964.4	967.6
Continuous phase density ρ_c (kg m^{-3})	998.4		
Density ratio $\frac{\rho_d}{\rho_c}$ (-)	0.95	0.97	0.97
Dispersed phase dynamic viscosity μ_d (Pa s)	19 10^{-3}	96.5 10^{-3}	339.5 10^{-3}
Continuous phase dynamic viscosity μ_c (Pa s)	1.01 10^{-3}		
Viscosity ratio $\frac{\mu_d}{\mu_c}$ (-)	18.8	95.4	335.6
Refractive index (-)	1.400	1.402	1.402
Interfacial tension for 1%wt. surfactant (mN m)	9.65	10.14	10.60